

BBA 41994

Identification of Q_{400} , a high-potential electron acceptor of Photosystem II, with the iron of the quinone-iron acceptor complex

Vasili Petrouleas^a and Bruce A. Diner^b

^a Nuclear Research Center, Demokritos, Aghia Paraskevi, Attiki (Greece) and ^b Institut de Biologie Physico-Chimique, 13, rue Pierre et Marie Curie, 75005 Paris (France)

(Received September 3rd, 1985)

(Revised manuscript received January 30th, 1986)

Key words: Photosystem II; Quinone-iron acceptor complex; Q_{400} ; ESR; Mössbauer spectroscopy; (*C. reinhardtii*)

Measurements of the area bounded by the variable fluorescence induction curve and the maximum fluorescence yield as a function of redox potential led I. Ikegami and S. Katoh ((1973) *Plant Cell Physiol.* 14, 829–836) to propose the existence of a high-potential electron acceptor, Q_{400} ($E_{m7.8} = 360$ mV), associated with Photosystem II (PS II). We have generated the oxidized form of this acceptor (Q_{400}^+) using ferricyanide and other oxidants in thylakoid membranes isolated from a mutant of *Chlamydomonas reinhardtii* lacking Photosystem I and the cytochrome b_6/f complex. Q_{400}^+ was detected by a decrease in the extent of reduction of the primary quinone electron acceptor, Q_A , in a low-intensity light flash exciting PS II reaction centers only once. EPR measurements in the presence of Q_{400}^+ indicated the presence of new signals at $g = 8, 6.4$ and 5.5 . These disappeared upon illumination at 200 K or upon reduction with ascorbate. Mössbauer absorption attributed to the Fe^{2+} of the Q_A-Fe^{2+} acceptor complex of PS II disappeared upon addition of ferricyanide due to the formation of Fe^{3+} . The Fe^{2+} signal was restored by subsequent addition of ascorbate. All of these spectroscopic signals show similar pH-dependent ($n = 1$) midpoint potentials (approx. -60 mV/pH unit) and an $E_{m7.5} = 370$ mV. We assign the EPR signals to the Fe^{3+} state of the quinone-iron acceptor. Electron transfer to the Fe^{3+} is responsible for the decrease in Q_A reduction upon single-hit flash excitation. The properties of the Fe^{3+}/Fe^{2+} redox couple are consistent with those of Q_{400}^+/Q_{400} and we conclude that the iron of the Q_A-Fe acceptor complex is responsible for this species.

Introduction

The fluorescence yield of chlorophyll increases non-linearly with the photoreduction of the primary quinone electron acceptor, Q_A , of Photosystem II (PS II) during actinic illumination of dark-adapted chloroplasts or algae in the presence

of DCMU [1]. The area bounded by the $I \times t$ -dependent (light intensity \times time) variable fluorescence yield (fluorescence induction curve) and the maximum fluorescence yield is, however, a linear function of the concentration of reducible acceptor available to the reaction center before the DCMU block [2].

Ikegami and Katoh [3] have reported that this area could be observed to increase up to 2-fold with increasing redox potential, showing a single electron Nernst curve with a midpoint potential of 360 mV at pH 7.8. This increased area thus titrated at a potential well above that of Q_A/Q_A^- ($E_{m7} = 0$

Abbreviations: Chl, chlorophyll; Cyt, cytochrome; DCMU, diuron, 3-(3,4-dichlorophenyl)-1,1-dimethylurea; PS I, Photosystem I; PS II, Photosystem II; Hepes, 4-(2-hydroxyethyl)-1-piperazineethanesulfonic acid; Mes, 4-morpholineethanesulfonic acid; Mops, 4-morpholinepropanesulfonic acid; Ches, 2-(*N*-cyclohexylamino)ethanesulfonic acid.

V, for a discussion see Refs. 4 and 5) and was attributed to an additional Photosystem II (PS II) acceptor, R, now known as Q_{400} , located between the reaction center and the site of DCMU inhibition. Ikegami and Katoh [3] also showed that if DCMU were added before the oxidant, ferricyanide, instead of in the reverse order, then the increase in the area above the fluorescence induction curve was largely inhibited, indicating that DCMU prevented the oxidation of Q_{400} .

These results were extended by Bowes et al. [6] who demonstrated that the midpoint potential of Q_{400} was pH-dependent (-60 mV/pH unit) and that its reduction occurred within $5 \mu\text{s}$ of actinic flash excitation of PS II reaction centers at room temperature. Because of its rapid reduction, this acceptor and Q_A provide two oxidizing equivalents, both available to the PS II reaction center in microsecond times. Together they have been suggested to be responsible for a double advance of the O_2 -evolving site upon microsecond flash excitation under oxidizing conditions [7,8] and double turnover of the reaction center even upon excitation with laser flashes of 300 ns lifetime [8].

The presence of this acceptor has been detected only by indirect means, i.e., fluorescence yield and double turnover of the O_2 -evolving site. Q_{400} has thus not been identified chemically, though a number of authors have proposed identifying it with ferricyanide [9] or a quinone [10], Wraight [11] has recently argued that Q_{400} is not a bound ferricyanide either, but an endogenous component whose oxidation decreases the binding affinity of DCMU at high pH. A consequent DCMU-induced midpoint potential increase for Q_{400}^+/Q_{400} [11] would explain the blockage by this inhibitor of Q_{400} oxidation, in the presence of ferricyanide as originally reported by Ikegami and Katoh [3]. In this paper we have taken this identification a step further and we will attempt to demonstrate convincingly that Q_{400} is the PS II acceptor-side Fe(II) which is closely associated with the primary quinone acceptor, Q_A .

Materials and Methods

Photosynthetic membranes

Mutant strains of *Chlamydomonas reinhardtii* were grown on Tris-acetate-phosphate medium [12]

in dim light at 25°C and harvested in the late logarithmic phase of growth. Iron ($\text{FeSO}_4 \cdot 7\text{H}_2\text{O}$) was left out of the trace metals solution of the medium and was replaced by $^{57}\text{FeBr}_3$ ($2 \mu\text{M}$ final concentration in medium). The latter was prepared by dissolving $^{57}\text{Fe}_2\text{O}_3$ (purchased from Oak Ridge National Laboratory) in concentrated HBr. The solution was heated to boiling and evaporated to dryness. The residue ($^{57}\text{FeBr}_3$) was taken up in water to make a stock solution at a final concentration of 10 mM.

The mutants used were strains F14.16.1 and AC206M18, isolated by Pierre Bennoun, and devoid of the PS I reaction center and the cytochrome b_6/f complex. These mutants were chosen to minimize the presence of photosynthetic iron-protein complexes other than those associated with the PS II reaction center. The two strains appeared to be identical according to their polypeptide profiles on SDS-polyacrylamide gel electrophoresis.

Thylakoid membranes were prepared from these mutants as described by Diner and Wollman [13] and suspended in the indicated buffers. Thylakoid membrane fragments (BBY * particles) were prepared from market spinach with some modifications [14,15] of the original procedure [16]. These membrane preparations were stored at -80°C until use.

Optical spectroscopy

Optical spectroscopy measurements were performed at 25°C on a flash-detection spectrophotometer similar to that described by Joliot et al. [17]. Actinic flashes were provided by both a xenon flash lamp (EG&G model FX 199U, $2 \mu\text{s}$ width at half-height) filtered by a red high band-pass filter (Schott RG 5, > 660 nm) and a dye laser (Candela Co. model SLL-150, 600 ns total duration, dye Oxazine 720, $\lambda_{\text{max}} = 693$ nm). For measurements in the ultraviolet the photodiodes were protected from actinic illumination by Corion solar blind filters (SB 300F).

Mössbauer spectroscopy

Mössbauer measurements were obtained using a constant acceleration spectrometer and a ^{57}Co -

* BBY, Berthold, Babcock and Yocum (see Ref. 16).

(Rh) source. Sample holders were disk-shaped with a maximum sample capacity of 1.6 ml. For measurements where illumination prior to the experiment was desired, the sample was placed in 1 mm thick holders which were laid on the bottom of a vial, half immersed in the cooling liquid (frozen acetone). A Cu-constantan thermocouple placed in a similar holder adjacent to the sample holders was used to monitor the temperature variation during illumination. Continuous actinic illumination, provided by a 300 W projector lamp, was filtered through 2.5 cm of a saturated CuSO_4 solution.

Electron spin resonance spectroscopy

EPR measurements were obtained with a Bruker ER 200D-SRC spectrometer equipped with an Oxford ESR 9 cryostat slightly modified to allow efficient purging of the sample with the cooling liquid. Thermal gradients were occasionally monitored by placing a Au (0.03% in Fe) vs. Ag-normal thermocouple in direct contact with the upper part of the sample above the sensitive area of the cavity. Gradients in the measurements reported did not exceed 1 K. Samples were placed in 3 mm ID quartz tubes. Illumination was normally performed inside the cavity using the same continuous light source as above. As indicated by the extent of reduction in the $g = 8$ signal size (at 200 K, see below) about 90% of the centers could be excited by 2.5 min illumination (50 s for every 120° rotation of the sample). The spectra were transferred via a Kikusui digital storage oscilloscope (model DSS6521) to a Tektronix microcomputer (model 4052A) which was connected to a Calcomp digital plotter (model 84). No signal averaging was employed in these spectra.

Redox-potential measurements

Redox potentials (E_h) are expressed relative to the standard hydrogen electrode at 25°C. For optical spectroscopy experiments, redox potentials were measured using platinum and calomel electrodes (Radiometer P101 and K401, respectively) connected to a Radiometer PHM84 Research pH meter. For Mössbauer and EPR experiments, redox potentials were measured using Metrohm combined microelectrodes ($\text{Ag}|\text{AgCl}|\text{KCl}$ 3 M) connected to a Dana microvoltmeter (model 5330).

A solution of 10 mM $\text{K}_3\text{Fe}(\text{CN})_6$ /10 mM $\text{K}_4\text{Fe}(\text{CN})_6$ /100 mM KCl was taken to have an $E_h = 436$ mV at 25°C [6].

$\text{K}_4\text{W}(\text{CN})_8 \cdot 2\text{H}_2\text{O}$ was synthesized according to the procedure of Leipoldt et al. [18] and oxidized electrolytically.

Results

Optical spectroscopy

Measurements of the kinetics of fluorescence induction in the presence of DCMU [3] or of the increase in fluorescence yield during a 20 μs xenon flash in the absence of this inhibitor [6] indicated the presence of an additional acceptor, Q_{400} available to the reaction center on a time-scale less than 5 μs (25°C) and located prior to the DCMU block.

One would predict, based on these observations, that PS II reaction centers, undergoing a single photoreaction under oxidizing conditions where Q_{400}^+ is present, should show a lowered concentration of Q_A^- on a time-scale larger than 5 μs . Such a prediction is tested in Fig. 1.

Stock suspensions of F14.16.1 membranes (5 mg Chl/ml) were preincubated with 0.8 mM ascorbate in 50 mM Hepes-KOH at 0°C for at least 15 min (for justification see below). They were then diluted to 25 μg Chl/ml in the indicated buffers (Fig. 1) at pH values 6.34 and 7.44 and incubated in darkness at 25°C for 15 min in the presence of 0.1 mM $\text{K}_3\text{Fe}(\text{CN})_6$ and varying concentrations of $\text{K}_4\text{Fe}(\text{CN})_6$ to vary the redox potential. The ferricyanide concentration was kept constant so as to maintain invariant for all samples any small amount of quenching of actinic excitation.

Following incubation, the samples were either used directly or made 20 μM in DCMU. Measurements of light-induced Q_A^- formation were made after 1-min incubation in the dark in the presence of inhibitor. Actinic excitation was provided first by a non-saturating xenon flash exciting approx. 30% of the PS II centers (producing single hits in 85% of these) followed 300 ms later by a saturating laser flash and 6 s after that by a second saturating laser flash.

For experiments performed in the presence of DCMU, the absorption increase measured at 320

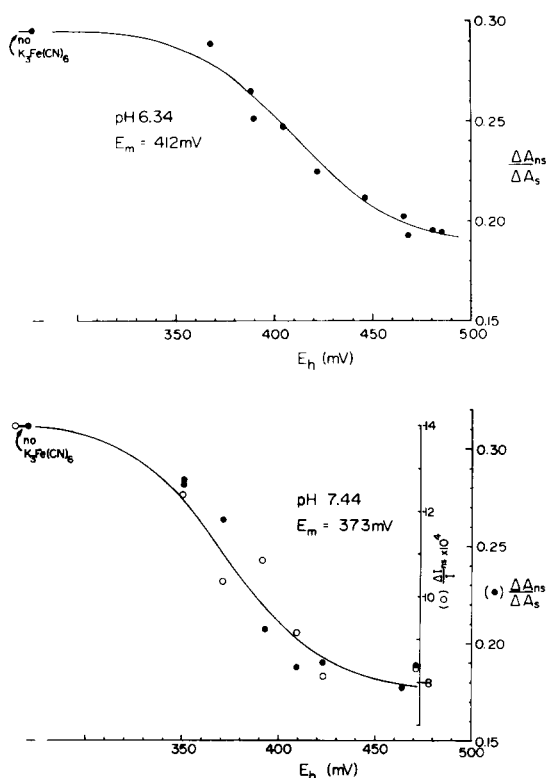


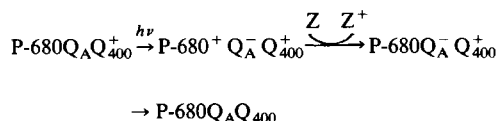
Fig. 1. Absorbance change at 320 nm induced by a xenon flash (hitting 30% of the PS II centers) as a function of redox potential in the presence and absence of DCMU. F14.16.1 membranes were suspended (25 μ g Chl/ml) in 50 mM Mes-KOH (pH 6.34) (upper) or 50 mM Hepes-KOH (pH 7.44) (lower each containing 0.1 mM $K_3Fe(CN)_6$ and variable concentrations of $K_4Fe(CN)_6$. After 15 min incubation in the dark (25°C) at the indicated potentials, samples were measured with (●) or without (○) 20 μ M DCMU following an additional 1 min dark incubation. The non-saturating flash was followed by a first saturating flash after 300 ms and a second after 6 s. The data with DCMU present are expressed as the ratio of the ΔA_{320} produced by the non-saturating and by the second saturating flash. That without DCMU is simply the non-saturating flash signal ($\Delta I/I$). $\Delta I/I$ was measured between 5 and 275 ms after the actinic flash.

nm (close to peak for $Q_A^- - Q_A$, Ref. 19) for the first non-saturating flash was divided by that of the second of the two saturating flashes. This ratio is plotted as a function of redox potential in Fig. 1. The ratio of the two signals was taken to eliminate any eventual interference from Q_B^- initially present in the dark and variations in pipetting of the thick membrane suspension. A plot (not shown) of the second saturating flash yield as a function of

redox potential showed it to increase by less than 10% with redox potential over the potential range studied. For the titration performed in the absence of DCMU, only the first non-saturating flash yield is indicated.

Fig. 1 shows that as the redox potential increases through the range in which Q_{400} becomes oxidized, the absorbance increase (ΔA_{320}) induced by the single-hit flash decreases by approx. 35% with an apparent midpoint potential of 412 mV at pH 6.34 and 373 mV at pH 7.44 consistent with the midpoint potential and its pH-dependence reported for Q_{400} [6].

Thus the presence of Q_{400}^+ decreases the amount of Q_A^- stabilized in a single-hit flash. This decrease probably arises from oxidation of Q_A^- by Q_{400}^+ as indicated in the following scheme:



However, a scheme in which Q_A and Q_{400}^+ operate in parallel cannot yet be excluded.

The decrease in $\Delta A_{320\text{ nm}}$ with increasing potential indicates that the extinction coefficient at 320 nm for $Q_{400} - Q_{400}^+$ is less than that for $Q_A^- - Q_A$. The complete spectrum of the light-induced absorbance change (not shown) indicates that in the absence of Q_{400}^+ this spectrum is composed largely of the PS II acceptor-side change $Q_A^- - Q_A$ [19] and a donor side change $M^+ - M$ [20] arising from the O_2 -evolving site. Measurements at 285 nm, an isosbestic point for $Q_A^- - Q_A$, indicate a signal for $M^+ - M$ about 35% of the total signal measured at 320 nm (without correction for particle flattening [21]). The extinction coefficient for $M^+ - M$ is approx. the same at 320 and at 285 nm (after correction for flattening) [20]. Applying the differential flattening factors of Pulles [21] ($\Delta E_{\text{sol}}/\Delta E'_{285\text{ nm}} = 2.3$; $\Delta E_{\text{sol}}/\Delta E'_{320\text{ nm}} = 1.6$) to our results, $M^+ - M$ would contribute to about 50% of the ΔA_{320} . Thus the decrease in Q_A^- formed in the presence of Q_{400}^+ would correspond to about 80% of the PS II centers if the extinction coefficient for $Q_{400} - Q_{400}^+$ were zero at 320 nm. If this extinction coefficient were positive at this wavelength, then the decrease in Q_A^- formed would be greater still.

We found that preincubation of the concentrated thylakoid membranes with ascorbate (see above) was necessary to obtain maximum signal amplitude of the ΔA_{320} in the absence of ferri- and ferrocyanide. Failure to add ascorbate lowered this signal by about 20% with or without DCMU, suggesting that some Q_{400}^+ was already present prior to the addition of the exogenous oxidants or reductants. This observation was confirmed by EPR measurements (see below Fig. 2c).

Electron spin resonance spectroscopy

The measurements of Q_{400} in the previous section and those described by previous authors are indirect indicators of the presence of this species. The use of thylakoid membranes lacking the cytochrome b_6/f complex and the PS I reaction

center made possible a direct search for EPR signals corresponding to Q_{400}^+ .

Fig. 2a shows an EPR spectrum of F14.16.1 membranes at pH 7.5 oxidized in the dark to a potential, E_h of approx. 460 mV. New peaks not present or present with reduced intensity in untreated samples are apparent at $g = 8$ and 5.5–6.4. Also shown is the spectrum following illumination at 200 K (limiting PS II to one or two turnovers) and the difference between the two. The difference spectrum obtained under these illumination conditions indicates that these same peaks are linked to redox changes occurring close to or within the PS II reaction center.

The $g = 8$ peak is quite strong and the $g = 6$ region is characterized by a prominent derivative-shaped contribution at $g = 5.5$ and a peak at

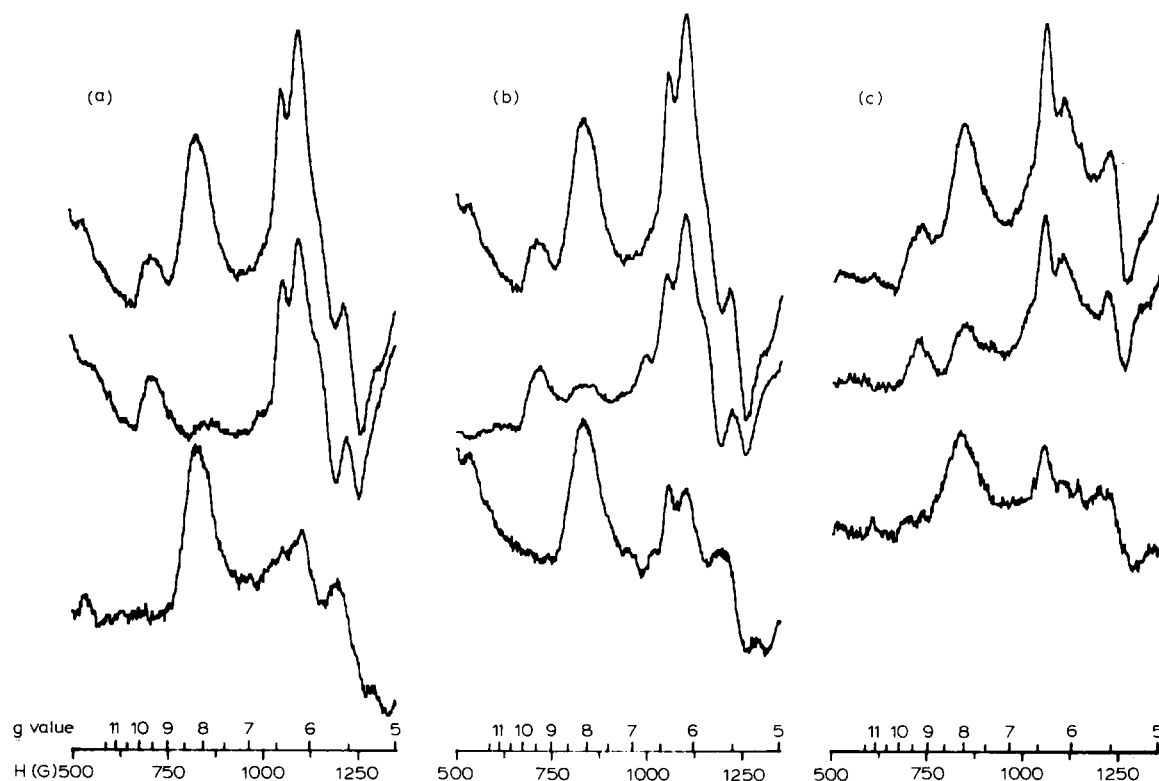


Fig. 2. EPR spectra of F14.16.1 membranes (5 mg Chl/ml) in 50 mM Hepes-KOH pH 7.5 showing reversible formation of signals at $g = 8$, 6.4 and 5.5. (a) Dark-adapted sample (upper) oxidized by 2 mM ferricyanide ($E_h = 455$ mV) followed by illumination at 200 K for 3 min (middle). (b) Dark-oxidized sample ($E_h = 455$ mV, upper) followed by addition of sodium ascorbate ($E_h = 260$ mV, middle). (c) Dark-adapted sample oxidized by air (upper) followed by illumination at 200 K (middle). The lower traces are the difference spectra between the upper and middle traces. Instrument settings: temperature 4.5 K, microwave power 5 mW, microwave frequency 9.42 GHz, modulation amplitude 32 G; the g -scale is approximate.

$g = 6.4$, as well as weaker features in between. There is some variability in the relative intensities of these signals. In general the signal at $g = 5.5$ is accompanied by a peak at $g = 6.4$. We have also observed a $g = 8$ signal in BBY preparations from spinach [14–16] at pH 5.9. Nugent and Evans [22] have observed in subchloroplast particles, in the presence of 5 mM ferricyanide, EPR signals at $g = 8.1$ and in the $g = 6$ region which decreased upon illumination at 5 K. While no interpretation was given, these signals are undoubtedly the same as those that we describe in detail here.

Following illumination at 200 K (Fig. 2a), dark adaptation at ambient temperature for 15 min restores practically all of the original signals indicating reversibility of redox behavior. These signals can also be observed (Fig. 2c) to arise spontaneously in the absence of $K_3Fe(CN)_6$ particularly at high pH (at least 7.5) under aerobic conditions or in the presence of H_2O_2 .

Reduction of a dark-oxidized sample with ascorbate to an E_h value of approx. 300 mV in the dark induces similar changes (Fig. 2b) to those observed upon illumination. The simplest explanation (supported by Mössbauer data, see below) for the latter observation (Fig. 2a) is that PS II, like ascorbate, has reduced the oxidized species responsible for this signal. However, magnetic coupling to a PS II-photogenerated radical (e.g., Q_A^-) could explain part of the disappearance.

Redox titration at pH 7.5 (Fig. 3) indicates that both signals at $g = 8$ and $g = 5.5$ titrate with the same midpoint potential. The experimental points are fit reasonably well by a Nernst curve with $n = 1$ and an $E_{m7.5}$ value of approx. 370 mV.

Titration of the $g = 8$ signal at pH 5.9 (Fig. 3) requires higher potentials ($E_{m5.9} = 475 \pm 20$ mV). This peak is however much broader than that at pH 7.5. Light-insensitive peaks at $g = 6$ and 4.3 titrate within the same range making the detection of the $g = 5.5$ and 6.4 signals ambiguous.

Fig. 4 shows the effect of the order of addition of DCMU and ferricyanide at 20°C on the amplitudes of the EPR signals in spinach BBY preparations at pH 8.5. Incubation with 1.2 mM $K_3Fe(CN)_6$ for 12 min followed by 1 min in 0.2 mM DCMU (Fig. 4c) gave a $g = 8$ signal 3.3-times larger than that obtained by 1 min incubation with 0.2 mM DCMU followed by 12 min in 1.2

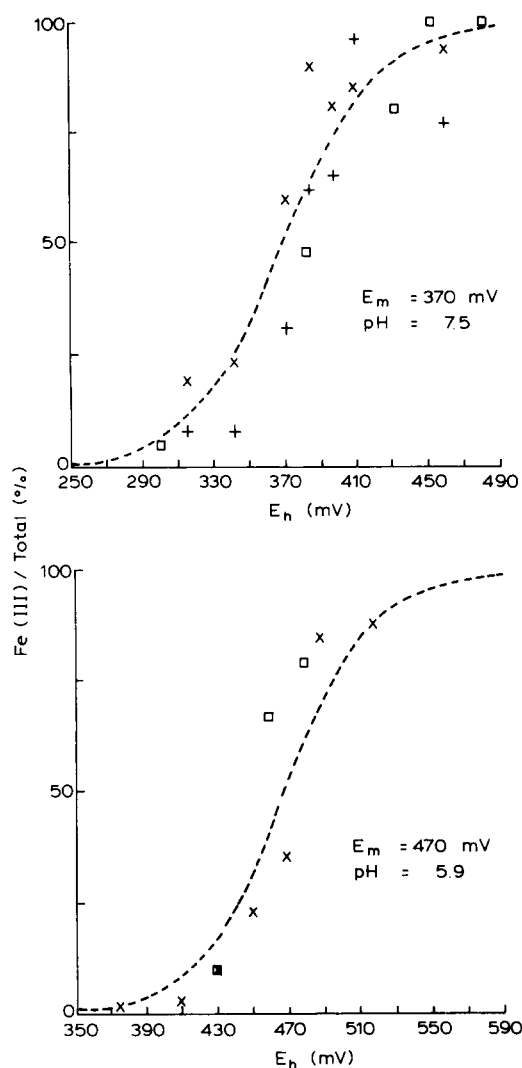


Fig. 3. Redox titrations of EPR signals at $g = 8$ (\times) and $g = 5.5$ ($+$) and of the percent loss of the Mössbauer $^{57}Fe^{2+}$ absorption (\square) arising from the quinone-iron acceptor complex. The EPR spectra were recorded under the conditions of Fig. 2. The Mössbauer spectra were recorded under the conditions of Fig. 5. The buffers used were 50 mM Hepes-KOH (pH 7.5) and 50 mM Mes-KOH (pH 5.9). The dashed lines are Nernst curves ($n = 1$).

mM $K_3Fe(CN)_6$ (Fig. 4b). Incubation of the membranes for 13 min at 20°C but with no additions (Fig. 4a) gave no formation of EPR signals. DCMU thus appears to diminish the accessibility or action of the oxidant. In both cases (Fig. 4b and c) the signals generated are largely eliminated by illumination at 100 K, indicating

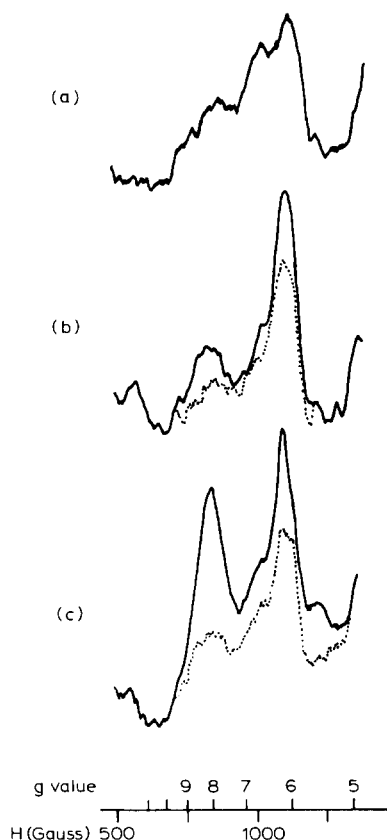


Fig. 4. Effect of the order of addition of $K_3Fe(CN)_6$ and DCMU on the amplitudes of the EPR spectra of spinach BBY preparations. The solid line spectra were obtained following treatment in the dark. The dotted line spectra were obtained following illumination for 3 min, at 100 K inside the EPR cavity. (a) Untreated sample incubated for 13 min at 20°C and then frozen to 77 K (the dark and illuminated spectra coincide); (b) incubation at 20°C with 0.2 mM DCMU for 1 min followed by 1.2 mM $K_3Fe(CN)_6$ for 12 min, then frozen to 77 K; (c) incubation at 20°C with 1.2 mM $K_3Fe(CN)_6$ for 12 min followed by 0.2 mM DCMU for 1 min, then frozen to 77 K. The BBY preparations were used at 5 mg Chl/ml in 58 mM Ches buffer, final pH 8.5 and were diluted immediately before use from a stock solution at pH 5.9 to avoid spontaneous oxidation of Fe^{2+} . DCMU was added from a stock solution containing DMSO and water. The final concentration of DMSO was 0.2%. The EPR instrument settings were as in Fig. 2, except that the temperature was 5.3 K.

that they arise from a species to the reaction center side of the DCMU inhibition site. The importance of the order of addition of DCMU and ferricyanide is analogous to that reported by Ikegami and Katoh [3] and by Wraight [11] for fluorescence measurements of Q_{400}^+ .

The position and pH-dependence of the midpoint potential of the $g = 8$ signal, the dependence of the signal amplitude on the order of addition of ferricyanide and DCMU and the detection by the $g = 8$ signal of a redox species having a close association with the acceptor side of PS II (see also next section) prior to the DCMU binding site make this signal an almost certain indicator for Q_{400} , which shares all of these characteristics.

The signals observed here are in a region of the EPR spectrum in which one would expect to find high spin Fe^{3+} . That this assignment is indeed justified will be shown in the next section. Given this likely assignment, the two sets of signals $g = 8$ and $g = 6.4-5.5$ probably represent different local symmetries at the Fe^{3+} site with the signals in the $g = 6$ region having near axial symmetry. The signal at $g = 8$ is indicative of considerably more rhombic symmetry.

Apart from the resonances cited above, an increase in the $g = 4.3$ peak is observed following certain treatments – e.g., long aerobic oxidation. This resonance appears on top of a strong impurity signal in this region and cannot be studied accurately. The appearance of this signal may be related to irreversible changes.

Mössbauer spectroscopy

An Fe^{2+} has been shown to be magnetically coupled to the reduced form of the primary plastoquinone acceptor, Q_A^- . The $Q_A^- - Fe^{2+}$ complex has EPR [23,24] and Mössbauer [25] spectral properties similar to those observed in purple non-sulfur photosynthetic bacteria (Refs. 26, 27 and 28, respectively). By analogy with *Rhodospseudomonas viridis* the distance between Q_A and the Fe^{2+} is probably of the order of 0.7 nm, with the latter located midway between Q_A and the secondary acceptor quinone, Q_B [29]. Should this iron be oxidizable to Fe^{3+} , it would be a likely candidate for Q_{400} .

A description as well as a quantitative account of the ^{57}Fe Mössbauer spectra of PS II particles from *Chlamydomonas* has been presented earlier [30]. A typical spectrum of a membrane sample from *Chlamydomonas* mutant F14.16.1 is shown in Fig. 5. A stick diagram shows the approximate positions and identification of the various components each characterized by a doublet of absorp-

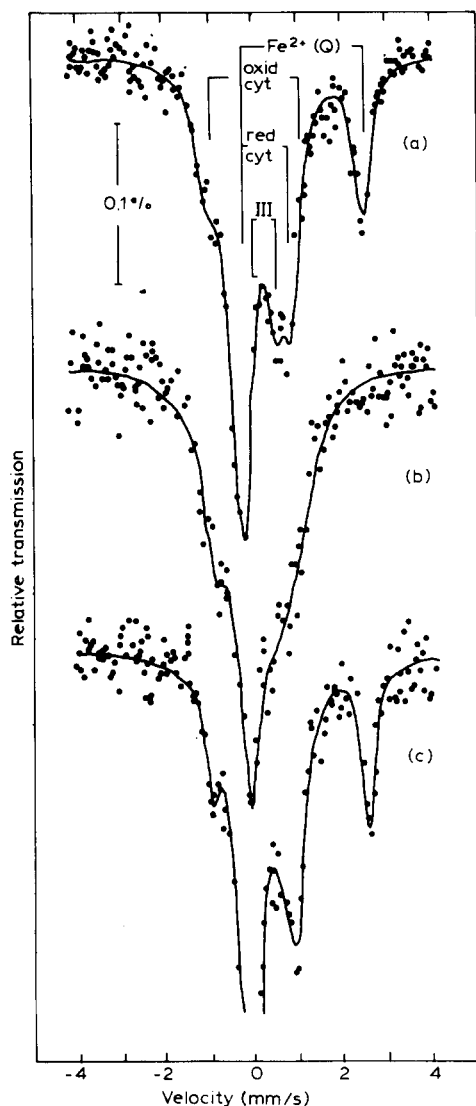


Fig. 5. Mössbauer spectra of F14.16.1 membranes (8 mg Chl/ml) in 50 mM Hepes-KOH (pH 7.5) recorded at 85 K. The solid lines are least-squares computer fits using Lorentzian lineshapes. The stick diagram identifies the various components: the Fe^{2+} of the quinone-iron acceptor complex and the oxidized and reduced forms of cytochrome *b*-559; (a) untreated sample; (b) sample oxidized to $E_h = 450$ mV by addition of 0.5 mM $\text{K}_3\text{Fe}(\text{CN})_6$; (c) sample oxidized to $E_h = 450$ mV and then reduced to 300 ± 20 mV by the addition of 0.7 mM sodium ascorbate.

tion peaks. These components are specifically associated with PS II as they are present in PS II reaction center particles [25] and absent in a mutant lacking the reaction center of this photo-

system. The assignment of the various components, based on redox titration of the Mössbauer and optical signals, will be described elsewhere. The main difference (Fig. 5) from the spectra of PS II particles [25,30] is the presence of a significant reduced cytochrome contribution due most probably to high-potential cytochrome *b*-559 in the membranes. The poorly resolved component in the middle, labelled component III as in earlier spectra [25], may have resulted from aerobic oxidation of Fe^{2+} to Fe^{3+} (see Fig. 2c). For the purpose of the present study, it is important to note that the right peak of the Fe^{2+} is well separated from all other contributions in the spectrum. Determinations of the extent of the Fe^{2+} oxidation will be based on the amplitude of this peak.

Fig. 5 shows the effect of addition, to membranes, of 0.5 mM $\text{K}_3\text{Fe}(\text{CN})_6$ which raises the potential, E_h , to approx. 450 mV. Pronounced changes occur in the spectrum. The most notable of these is the disappearance of the Fe^{2+} contribution. Measurements in *Chlamydomonas* PS II particles using $\text{K}_3\text{W}(\text{CN})_8$ as oxidant indicate that the decrease in the Fe^{2+} signal is accompanied by new absorption intensity in the range 0–0.5 mm/s. This absorption is not well defined, however, due either to relaxation effects or to a heterogeneity of sites. It is nonetheless compatible with the formation of high spin Fe^{3+} . In Fig. 5 the central part of the spectrum is complicated by the ferri-/ferrocyanide contributions and also by the expected oxidation of the reduced cytochrome contribution to low-spin Fe^{3+} , showing relaxation broadening at this temperature.

Addition of 0.7 mM sodium ascorbate (Fig. 5c) to the oxidized sample reduces the redox potential to 300 ± 20 mV and restores the original spectrum. Practically all the Fe^{2+} is restored to the level of the original untreated signal. The spectrum of Fig. 5c differs from the one in Fig. 5a by the increase in the intensity of the central peak due to contribution from $\text{K}_4\text{Fe}(\text{CN})_6$. The lowest part of the peak has been omitted.

The oxidation of the iron exhibits an apparent pH dependence. Membranes suspended in Mes-KOH buffer pH 5.9 show very little oxidation of the Fe^{2+} at $E_h \approx 430$ mV, a potential at which practically all the Fe^{2+} is oxidized at pH 7.5. Full

oxidation of the Fe^{2+} at pH 5.9 can be observed by raising the potential above 500 mV while at $E_h = 470$ mV about 50% of the iron is oxidized. Approximate titrations of *Chlamydomonas* membranes suspended in Mops buffer pH 6.7 suggest an E_m value in the range of 410–430 mV.

The above results show that the Fe^{2+} can be reversibly oxidized over a redox potential range in which Q_{400} is known to titrate. This range shifts to higher potential as the pH is lowered. The percentage loss of Mössbauer absorption by the Fe^{2+} at several different potentials and pHs are indicated in Fig. 3 and shows reasonable agreement with the EPR data at pH 5.9 and 7.5.

The reversibility of the Fe^{2+} oxidation decreases drastically after treatments such as prolonged exposure to air or several freeze-thaw cycles following the oxidation. Irreversibly oxidized iron can be rereduced only after lowering the potential below 150 mV in a form with different Mössbauer parameters.

In addition to $\text{K}_3\text{Fe}(\text{CN})_6$, $\text{K}_3\text{W}(\text{CN})_8$ and H_2O_2 are also effective oxidants of the Fe^{2+} as observed by Mössbauer, EPR, and optical spectroscopy (ΔA_{320}). In addition, incubation of PS II particles with glucose-glucose oxidase in the air for several minutes induces considerable oxidation of the Fe^{2+} , probably due to formation of H_2O_2 .

The g -values (8 and 5.5) of the EPR signals and their redox behavior similar to that observed for the Mössbauer detectable ^{57}Fe , lead us to attribute them to the Fe^{3+} state of the iron of the PS II acceptor-side quinone-iron complex.

Discussion

Fe and Q_{400}

The iron of the PS II acceptor-side quinone-iron complex, as detected by the EPR and Mössbauer signals we attribute to it, shares with Q_{400} the following properties:

- similar midpoint potentials which increase with decreasing pH in a manner consistent with -60 mV/pH unit [3,6];
- association with the electron acceptor side of PS II, located between the primary reactants and the DCMU binding site [3,6];
- extent and/or rate of oxidation by ferricyanide inhibited by prior addition of DCMU [3,11];

– considering what we know about the distances and rates implicated in electron transfer in reaction centers from *Rps. viridis* [29], the close proximity of the iron to Q_A (probably 0.7 nm [29]) is consistent with rapid (less than 5 μs) electron transfer to Q_{400}^+ .

We conclude that Q_{400} and the acceptor-side iron are one and the same.

In contrast to this conclusion it has been suggested that Q_{400} might be ferricyanide itself oxidizing Q_A^- [9]. This suggestion was supported by the fact that all observations of Q_{400} had until then involved ferricyanide as oxidant. However, the EPR and Mössbauer signals we report here are indicative of high spin Fe^{3+} and thus are not consistent with this assignment, as ferricyanide is low spin. Also the Q_{400} -like behavior of the optical experiments of Fig. 1 and the EPR signals we attribute to Q_{400} can be induced in the absence of ferricyanide by air, $\text{K}_3\text{W}(\text{CN})_8$ or by H_2O_2 . Furthermore, the rate constant reported for oxidation of Q_A^- by this oxidant in the presence of DCMU [9] is much slower than that reported by Bowes et al. [6] for reduction of Q_{400}^+ . Finally, Wraight [11] has argued against a bound form of ferricyanide on the basis of the disappearance of Q_{400}^+ and its attendant inhibition of DCMU binding by addition of ferrocyanide.

Q_{400} has also been reported [10] to show a quinone-like spectrum with a flash-induced absorbance increase, peaking at 315 nm, and a bleaching, peaking at 275 nm. The 2-fold stimulation by $\text{K}_3\text{Fe}(\text{CN})_6$ of ΔA_{320} reported by Denenberg and Jursinic [10] is in contradiction with the ferricyanide-induced inhibition reported here. The $\pm \text{K}_3\text{Fe}(\text{CN})_6$ difference spectrum described in Ref. 10 is induced by a 3 μs xenon flash capable of producing a double turnover of PS II. As greater double turnover is observed in the reaction center than for O_2 evolution [8], one would then expect an additional donor-side contribution (other than S-states) as compared to our optical measurements. This additional contribution plus a possible electrochromic shift of the Q_A (or Q_B) spectrum by Fe^{3+} – Fe^{2+} might explain the spectrum of Denenberg and Jursinic [10].

In the optical experiment reported here, PS II centers are excited by a non-saturating flash delivering a single hit to 26% of the centers and two

or more hits to only 4.5% of the centers. If the extinction coefficient of $Q_{400} - Q_{400}^+$ were equivalent to that of $Q_A^- - Q_A$ at 320 nm ($12.5 \text{ mM}^{-1} \cdot \text{cm}^{-1}$, Ref. 15), as suggested in Ref. 10, then we would not have seen a decrease by ferricyanide of ΔA_{320} . Furthermore, we show that this decrease has a redox potential dependence equivalent to that of Q_{400} , arguing strongly that $\Delta \epsilon_{Q_{400} - Q_{400}^+} < \Delta \epsilon_{Q_A^- - Q_A}$. The exact fraction of centers affected by electron transfer to Q_{400}^+ cannot be estimated accurately, because the extinction coefficient of $Q_{400} - Q_{400}^+$ is unknown. However, if it is 0 or more, then at least 80% of the PS II centers are capable of photoreduction of Q_{400}^+ .

Other evidence suggests that not all centers show Q_{400} behaviour, Pierre Joliot (personal communication) and Bowes et al. [6] have pointed out that Ikegami and Katoh [3] may have overestimated the Q_{400}^+ concentration by overcorrecting for ferricyanide quenching of fluorescence. Bowes et al. [6] estimated the Q_{400} /QS II reaction center at 0.35 to 1. Using measurements of continuous light-induced C550 formation in the presence of DCMU, following preincubation $\pm K_3Fe(CN)_6$, Pierre and Anne Joliot (personal communication) estimated that only half the PS II centers were deficient in C550 in the single-hit phase of illumination (pH 6.5). Thus all centers may not show Q_{400} behavior despite the fact that all appear to contain iron – e.g. no apparent free semiquinone EPR signal ($g = 2.0044$) upon illumination of TSF II particles at 220 K, $E_h \approx +50 \text{ mV}$ [32]. Also in *Chlamydomonas* PS II reaction center particles no free semiquinone EPR signal is observed in 10 mM dithionite, pH 7.5, unless the iron is specifically extracted (in collaboration with T.K. Chandrashekar and G.T. Babcock, unpublished results).

Such heterogeneity might explain why, upon illumination at 200 K (not shown), only 20–30% of the Mössbauer Fe^{2+} absorption reappears (conditions of Fig. 5b). Other possibilities are a low probability for $Q_A^- - Fe^{3+}$ electron transfer at this temperature or the extremely high optical density of the Mössbauer sample. These alternatives are currently under investigation.

The EPR spectrum with peaks at $g = 8, 6.4$ and 5.5 cannot all arise from the same species. The $g = 6.4$ and 5.5 signals probably arise from an

Fe^{3+} component having largely axial symmetry, while that at $g = 8$ indicates more rhombic distortion. Two alternative resonances have also been reported for the $Fe^{2+} - Q_A^-$ EPR signal [24]. These are also observed in the present samples. The Mössbauer absorption due to Fe^{2+} exhibits asymmetric or broad lineshapes indicative of heterogeneity at the Fe^{2+} site, despite their homogeneous behavior upon redox titration (Fig. 3).

At least two forms of heterogeneity may exist among PS II centers which may have consequences for electron transfer involving the acceptor side quinones. One of these is the state of phosphorylation of reaction center polypeptides. In the case of *Chlamydomonas reinhardtii*, two PS II reaction center polypeptides (6 and D2) exist in both phosphorylated and non-phosphorylated forms [33]. The state of phosphorylation of membrane polypeptides has been shown to influence the stability of Q_B^- [34]. The degree of association of bicarbonate with PS II reaction centers may also be inhomogeneous. Bicarbonate depletion has been shown to diminish the rate of electron transfer between Q_A and Q_B [35], and the rate of reduction or concentration of Q_{400} [36], though this latter point is contested [31] and attributed to the presence of residual formate.

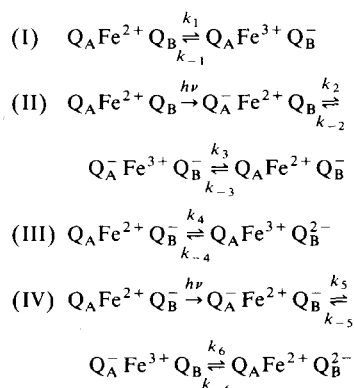
Finally, numerous reports exist in the literature of a heterogeneity of PS II reaction centers based upon the observation of a slow phase of the fluorescence induction curve in the presence of DCMU and in the absence of added oxidant. In addition, such heterogeneity is observed to increase upon fragmentation of chloroplasts [37]. Our observation of the aerobic oxidation of the Fe^{2+} of the quinone-iron complex, particularly at high pH (Fig. 2c) and that of Wraight [11], of inhibition of DCMU binding by Q_{400}^+ , could together account for some of these observations. Such aerobic oxidation could provide a simple explanation of reports [38,39] of double hitting in spinach chloroplast PS II at elevated, but not saturating DCMU concentrations in the absence of ferricyanide. Here, centers containing Q_{400}^+ and thus capable of a double turnover on a first saturating xenon flash would be resistant to DCMU. Centers with reduced Q_{400} would be inhibited and unable to evolve oxygen. Addition of DCMU effectively enriches the still-functioning population of centers

in those capable of double hitting. This phenomenon is not observed in algae [38,39] possibly for reasons of internal redox potential and pH.

Fe and Q_A - Q_B electron transfer

Having shown that the iron of the acceptor side quinone-iron complex has redox properties and a location consistent with Q_{400} , it is reasonable to ask what might be its physiological role, in particular whether it serves as a conduit for electrons from Q_A to Q_B [27]. The high apparent midpoint potential ($E_{m7.5} \approx 370$ mV) is not necessarily that operating in vivo where a negative charge on a neighboring semiquinone might shift downward the operating potential of the Fe^{3+}/Fe^{2+} couple.

One might imagine Fe involvement of the type indicated in the following sequence of reactions (ignoring protonation):



An equilibrium of the type indicated in (I) could account in part for the concentrations of Q_B^- observed in the dark in algal cells and chloroplasts, particularly under conditions of membrane polypeptide phosphorylation [34].

That of type (III) could account for centers having an unstable Q_B^- [40,41]. Reactions I and III could also explain in part what we have called spontaneous oxidation of Fe^{2+} to Fe^{3+} .

Reactions (II) and (IV) are the two single-electron transfer reactions between Q_A and Q_B . Depending on the relative rates (k_2 vs. k_3 and k_5 vs. k_6) the iron would either remain in the Fe^{2+} state (in a 'push-pull' type double-exchange mechanism) or become fully oxidized to Fe^{3+} .

The arguments in favor of iron participation in Q_A -to- Q_B electron transfer are listed below.

(a) Electron transfer probably occurs from Q_A^- to Fe^{3+} (this work) though no fast spectroscopic measurement has directly demonstrated this mechanism.

(b) Formate appears to slow electron transfer from Q_A^- to Q_{400} [31,36] and to slow turnover of PS II reaction centers [42]. The latter phenomenon probably reflects a slowing of Q_A to Q_B electron transfer, implying that the same route is involved in both cases.

(c) Loss of the acceptor side iron slows 2- to 3-fold Q_A^- -to- Q_B electron transfer in *Rhodospseudomonas sphaeroides* reaction centers [43].

(d) The iron is located midway between Q_A and Q_B [29].

(e) The iron is conserved in PS II reaction centers and those from purple photosynthetic bacteria.

The principal argument against iron participation, at least in photosynthetic bacteria, is that replacement of Fe^{2+} by Mn^{2+} or Zn^{2+} does not alter the rate of electron transfer from Q_A^- to Q_B [43,44]. As the redox properties of these three metal centers are quite different, one would have to claim, for the metal still to be involved, that the rate-determining step for this electron transfer does not involve a step in which the metal is implicated (e.g., Q_B binding or protonation).

A definitive conclusion on iron participation in Q_A - Q_B electron transfer would probably require the spectroscopic detection of a transient state involving Fe^{3+} either by rapid measurement or by trapping of intermediates at low temperature. Other possible approaches are closer examination of inhibited states (e.g., formate treatment), iron extraction and replacement by other metals, and ligand replacement by site-directed mutagenesis.

Acknowledgements

The authors gratefully acknowledge the support of the Mission des Biotechnologies (contract no. 82.V.1262) and of the CNRS (contract no. 980029). They also wish to thank Dr. Pierre Joliot for helpful discussions and Dr. Richard Malkin for his gift of $K_4W(CN)_8$.

References

- 1 Joliot, A. and Joliot, P. (1964) Compt. Rend. Acad. Sci. Paris 258, 4622-4625

- 2 Bennoun, P. and Li, Y.S. (1973) *Biochim. Biophys. Acta* 292, 162–168
- 3 Ikegami, I. and Katoh, S. (1973) *Plant Cell. Physiol.* 14, 829–836
- 4 Vermaas, W.F.J. and Govindjee (1981) *Photochem. Photobiol.* 34, 775–793
- 5 Diner, B.A. and Delosme, R. (1983) *Biochim. Biophys. Acta* 722, 443–459
- 6 Bowes, J.M., Crofts, A.R. and Itoh, S. (1979) *Biochim. Biophys. Acta* 537, 320–335
- 7 Velthuys, B. and Kok, B. (1977) *Proceedings of the Fourth International Congress on Photosynthesis* (Hall, D.O., Coombs, J. and Goodwin, T.W., eds.), pp. 397–407, The Biochemical Society, London
- 8 Jursinic, P. (1981) *Biochim. Biophys. Acta* 635, 38–52
- 9 Ghanotakis, D.F., Babcock, G.T. and Yerkes, C.T. (1983) *Arch. Biochem. Biophys.* 225, 248–255
- 10 Dennenberg, R.J. and Jursinic, P.A. (1985) *Biochim. Biophys. Acta* 808, 192–200
- 11 Wraight, C.A. (1985) *Biochim. Biophys. Acta* 809, 320–330
- 12 Gorman, D.S. and Levine, R.P. (1965) *Proc. Natl. Acad. Sci. USA* 54, 1665–1669
- 13 Diner, B.A. and Wollman, F.A. (1980) *Eur. J. Biochem.* 110, 521–526
- 14 Ford, R.C. and Evans, M.C.W. (1983) *FEBS Lett.* 160, 159–164
- 15 Rutherford, A.W., Zimmermann, J.L. and Mathis, P. (1984) *FEBS Lett.* 165, 156–162
- 16 Berthold, D.A., Babcock, G.T. and Yocum, C.F. (1981) *FEBS Lett.* 134, 231–234
- 17 Joliot, P., Béal, D. and Frilley, B. (1980) *J. Chim. Phys.* 77, 209–216
- 18 Leipoldt, J.G., Bok, L.D.C. and Cilliers, P.J. (1974) *Z. anorg. allg. Chem.* 407, 350–352
- 19 Van Gorkom, H.J., Thielen, A.P.G.M. and Gorren, A.C.F. (1982) in *Function of Quinones in Energy-Conserving Systems* (Trumpower, B.L., ed.), pp. 213–225, Academic Press, New York
- 20 Dekker, J.P., Van Gorkom, H.J., Brok, M. and Ouwehand, L. (1984) *Biochim. Biophys. Acta* 764, 301–309
- 21 Pulles, M.P.J. (1978) Thesis, Rijksuniversiteit Leiden
- 22 Nugent, J.H.A. and Evans, M.C.W. (1980) *FEBS Lett.* 112, 1–4
- 23 Nugent, J.H.A., Diner, B.A. and Evans, M.C.W. (1981) *FEBS Lett.* 124, 241–244
- 24 Rutherford, A.W. and Zimmermann, J.L. (1984) *Biochim. Biophys. Acta* 767, 168–175
- 25 Petrouleas, V. and Diner, B.A. (1982) *FEBS Lett.* 147, 111–114
- 26 Dutton, P.L., Leigh, J.S. and Reed, D.W. (1973) *Biochim. Biophys. Acta* 292, 654–664
- 27 Feher, G. and Okamura, M.Y. (1978) in *The Photosynthetic Bacteria* (Clayton, R., ed.), pp. 349–386, Plenum Press, New York
- 28 Boso, B., Debrunner, P., Okamura, M.Y. and Feher, G. (1981) *Biochim. Biophys. Acta* 638, 173–177
- 29 Deisenhofer, J., Michel, H. and Huber, R. (1985) *TIBS* 10, 243–248
- 30 Petrouleas, V. and Diner, B.A. (1984) in *Advances in Photosynthesis Research* (Sybesma, C., ed.), Vol. I, pp. 195–198, Martinus Nijhoff/Dr. W. Junk Publishers, Dordrecht, The Netherlands
- 31 Jursinic, P.A. and Stemler, A. (1984) *Biochim. Biophys. Acta* 764, 170–178
- 32 Klimov, V.V., Dolan, E., Shaw, E.R., Ke, B. (1980) *Proc. Natl. Acad. Sci. USA* 77, 7227–7231
- 33 Delepelaire, P. (1984) *EMBO J.* 3, 701–706
- 34 Jursinic, P.A. and Kyle, D.J. (1983) *Biochim. Biophys. Acta* 37–44
- 35 Jursinic, P., Warden, J. and Govindjee (1976) *Biochim. Biophys. Acta* 440, 322–330
- 36 Radmer, R. and Ollinger, O. (1980) *FEBS Lett.* 110, 57–61
- 37 Schreiber, U. and Pfister, K. (1982) *Biochim. Biophys. Acta* 680, 60–68
- 38 Diner, B.A. (1974) *Biochim. Biophys. Acta* 368, 371–385
- 39 Joliot, P. and Joliot, A. (1981) *Biochim. Biophys. Acta* 638, 132–140
- 40 Lavergne, J. and Etienne, A.L. (1980) *Biochim. Biophys. Acta* 593, 136–148
- 41 Boussac, A. and Etienne, A.L. (1982) *Biochim. Biophys. Acta* 682, 281–288
- 42 Stemler, A. and Jursinic, P. (1983) *Arch. Biochem. Biophys.* 221, 227–237
- 43 Debus, R.J., Okamura, M.Y. and Feher, G. (1985) *Biophys. J.* 47, 3a
- 44 Nam, H.K., Austin, R.H. and Dismukes, G.C. (1984) *Biochim. Biophys. Acta* 765, 301–308